2014 INTERNATIONAL OIL SPILL CONFERENCE

BIOTIC AND ABIOTIC OIL DEGRADATION AFTER THE *DEEPWATER HORIZON* DISASTER LEADS TO FORMATION OF RECALCITRANT OXYGENATED HYDROCARBONS: NEW INSIGHTS USING GC×GC

Christoph Aeppli,[1] Robert K. Nelson,[2] Catherine A. Carmichael,[2] David L. Valentine,[3] and Christopher M. Reddy[2]

[1] Bigelow Laboratory for Ocean Sciences, East Boothbay, Maine, USA
[2] Woods Hole Oceanographic Institution, Woods Hole, Massachusetts, USA
[3] UC Santa Barbara, Santa Barbara, California, USA

ABSTRACT 300229:

We found that biodegradation, as well as photooxidation, of Macondo well (MW) oil led to rapid formation of recalcitrant oxygenated hydrocarbons (OxHC) after the *Deepwater Horizon* disaster. These compounds, which appear to be an abundant product of natural oil degradation, are poorly characterized in terms of molecular composition. We used various bulk and molecular techniques to characterize the OxHC fraction of weathered MW oil. Furthermore, we compared the characteristic disappearance of various petroleum hydrocarbons to gain insights into on-going biotic, as well as abiotic, oil oxygenation processes, that ultimately determine the fate of petroleum hydrocarbons in the environment. We found that biodegradation as well as photooxidation was responsible for the observed degradation of alkanes and PAHs in MW oil. Furthermore, we identified labile as well as recalcitrant biomarker compounds; these labile biomarker compounds should be used with caution for oil fingerprinting.

INTRODUCTION:

Oil that is released into the environment after spills is altered though physical as well as (bio)chemical processes. These processes are often referred to as oil weathering. In a marine oil spill, physical processes consist of dissolution as well as evaporation, while the (bio)chemical processes are microbial degradation (biodegradation) as well as oxidation though sunlight (photooxidation) (Atlas 1981, Garrett *et al.* 1998, Nicodem *et al.* 1998, Prince and Walters 2007).

To assess the short- and long-term fate of petroleum hydrocarbons after an oil spill, it is important to identify and assess the relative importance of these weathering processes in the environment. Biodegradation and photooxidation, for example, seem to be very slow for the lingering oil of the 1989 *Exxon Valdez* oil spill after 16 years (Short *et al.* 2007). In contrast, for oil washed ashore after the 2010 *Deepwater Horizon* disaster in the Gulf of Mexico, extensive (bio)chemical weathering of oil was observed within 18 months (Aeppli *et al.* 2012).

New methods, such as comprehensive two-dimensional gas chromatography (GC×GC) advanced the potential to investigate processes that lead to chemical alternation of oil (Arey *et al.* 2007a, Arey *et al.* 2007b). The high chromatographic resolution of GC×GC also has advantages over one-dimensional GC (such as GC-MS) for oil fingerprinting (Frysinger *et al.* 2002, Eiserbeck *et al.* 2012).

The aim of this study was to identify physical, chemical, and microbial oil weathering processes in petroleum released after the *Deepwater Horizon* disaster. To this end, we analyzed a time series of oiled samples, collected along the coast of the northern Gulf of Mexico, using GC×GC and other analytical techniques. Whereas previous papers describe the formation of oxygenated hydrocarbons (OxHC) upon weathering, sequential biodegradation of alkane classes, and chemometric analysis of GC×GC data (Aeppli *et al.* 2012, Hall *et al.* 2013, Aeppli *et al.* 2014, Gros *et al.* 2014), this paper specifically investigates and summarizes how GC×GC allows for compound-specific degradation assessment of individual petroleum hydrocarbons, in order to gain insights into biotic and abiotic weathering processes.

METHODS:

Samples

Over 100 surface slicks, oil-soaked sand samples ("sand patties") and rock scrapings (oil scraped off rocks) were collected and analyzed (Figure 1). Some of these samples were previously described in Aeppli *et al.* (2012) and Hall *et al.* (2013); additional sand patties were collected in 2012. Surface slick samples were directly dissolved in dichloromethane (DCM) and dried with Na_2SO_4. Sand patties and rock scrapings were extracted with DCM / methanol (90/10 v/v) in centrifuge vials (3 extraction, with centrifugation in-between extraction). The sample and solvent amount was adjusted for the final oil concentration to be 10 to 50 mg L^{-1}.

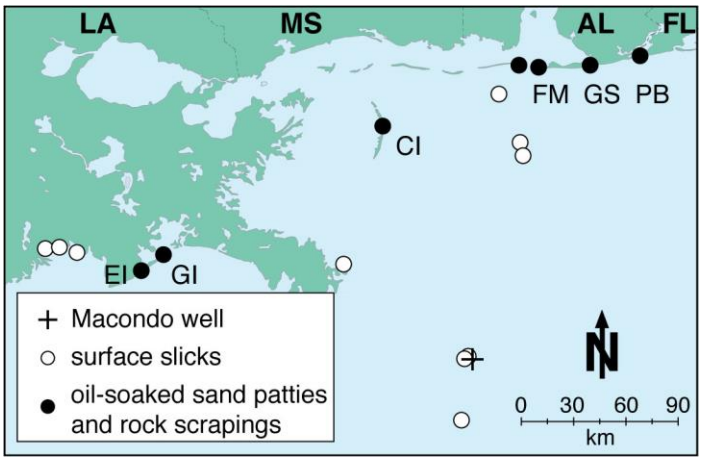

Figure 1. Map of sampling sites. Surface slicks (open circles) were collected May and June 2010, whereas sand patties and rock scrapings were collected at multiple time points from Perdido Beach (PB), Gulf Shores (GS), Fort Morgan (FM), Chandeleur Island (CI), Grand Isle (GI), and Elmer's Island (EI) between April 2011 through August 2012.

Analytical methods

Comprehensive two-dimensional gas chromatography coupled to flame ionization detection (GC×GC-FID) was performed as described in Hall *et al.* (2013). In brief, 1 µL sample volumes were injected in splitless mode into a GC×GC-FID system (Leco, Saint Joseph, MI), equipped with a Restek Rtx-1 first-dimension column (60 m, 0.25 mm ID, 0.25 µm film thickness) and SGE BPX-50 second-dimension column (1.5 m, 0.10 mm ID, 0.10 µm film). The inlet temperature was held at 300 °C and the carrier gas was hydrogen at a constant flow rate of 1.00 mL min^{-1}. The temperature program of the GC oven was 40 °C for 10 min, then ramped to 340 °C at 1.25 °C min^{-1} (held 5 min). The second-dimension oven had a constant offset of 5 °C relative to the main oven. A liquid-N_2 cooled two-stage modulator was used (Leco), and the modulation period was either 10 or 15 s.

One-dimensional gas chromatography (GC-FID) was also conducted (Aeppli *et al.* 2013), using a Hewlett-Packard 5890 Series II GC equipped with an Agilent DB-1MS capillary column (30 m, 0.25 mm I.D., 0.25 µm film) and operated at 5 mL min^{-1} H_2 carrier gas flow.

Thin-layer chromatography coupled to flame ionization detection **(**TLC-FID) was performed as described in Aeppli *et al.* (2012) using an Iatroscan MK-5 TLC−FID analyzer (Iatron Laboratories, Tokyo, Japan). Briefly, 1 to 5 µL of sample extracts were spotted on the base of a silica-gel sintered glass rod (Chromarod S III, Iatron Laboratories) which was then sequentially developed in hexane (26-min development time), toluene (12 min), and DCM/methanol 97/3 (5 min).

RESULTS/DISCUSSION:

Identification of MW oil in samples

To confirm that the investigated samples were MW oil, we used biomarker analysis (petroleum fingerprinting) methods (Wang *et al.* 2006), with ratios described earlier (Carmichael *et al.* 2012). GC×GC-FID led to excellent separation of individual petroleum hydrocarbon compounds including biomarkers (Figure 2).

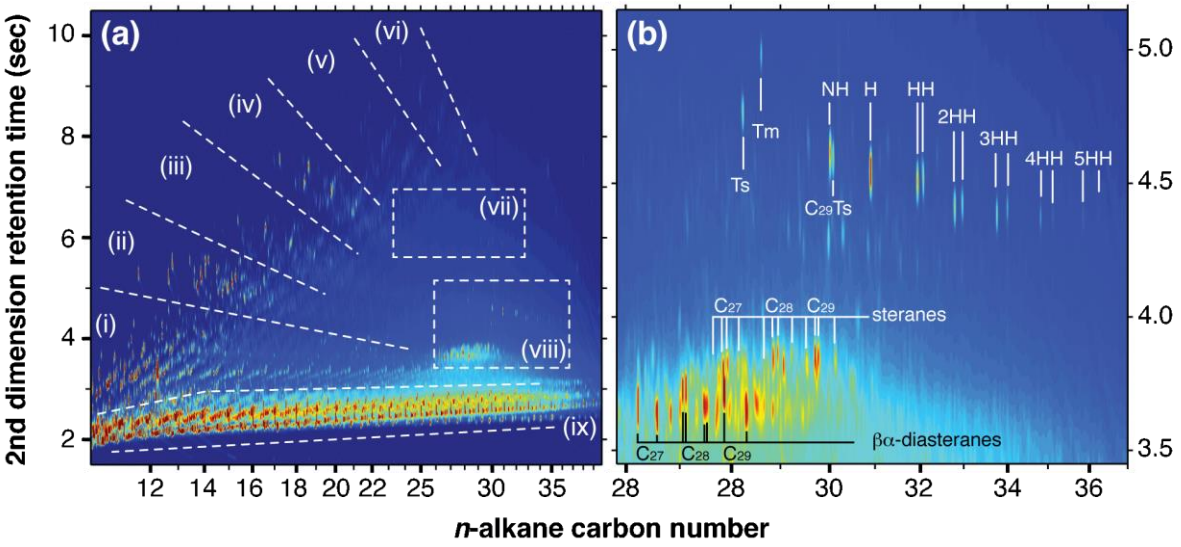

Figure 2. GC×GC chromatogram of Macondo well (MW) oil. The x-axis separates compounds according to retention on the apolar first-dimension column, whereas the second-dimension column (y-axis) separates according to polarity. **(a)** The whole two-dimensional chromatogram demonstrates grouping of compounds with similar physical properties in similar spaces of the GC×GC chromatogram. The indicated regions are *(i)* alkylbenzenes, *(ii)* naphthalenes and benzothiophenes, *(iii)* fluorenes, *(iv)* phenanthrenes and dibenzothiophenes, *(v)* fluoranthenes, *(vi)* chrysenes, *(vii)* triaromatic steroids, *(viii)* hopanes, steranes, and diasteranes, and *(ix)* saturated hydrocarbons. **(b)** An enlargement of the hopane and (dia)sterane region is given. The main hopane peaks are: 17α(*H*),21β(*H*)-hopane (H), homohopanes (HH through 5HH), C_{27}-hopanes (Ts, Tm), and 30-norhopane (NH).

The majority of the oil samples were identified as MW oil. The relative distribution of hopanoids and (dia)steranes of all surface slicks, sand patties, and rock scrapings was the same as for the MW oil (Aeppli *et al.* 2012). This can be seen by visual comparison (Figure 3), but was also confirmed quantitatively using biomarker ratios. A sub-set of samples, however, did not match the MW signature. These samples were visually different from sand patties or rock scraping, but were sand-free and asphalt-like bricks of 5 to 10 cm diameter, collected mostly along the shores of Grand Isle and Elmer's Island (LA). The sterane-to-hopane ratio and diasteranes-to-sterane ratios were especially different than the MW-type samples (Aeppli *et al.* 2014).

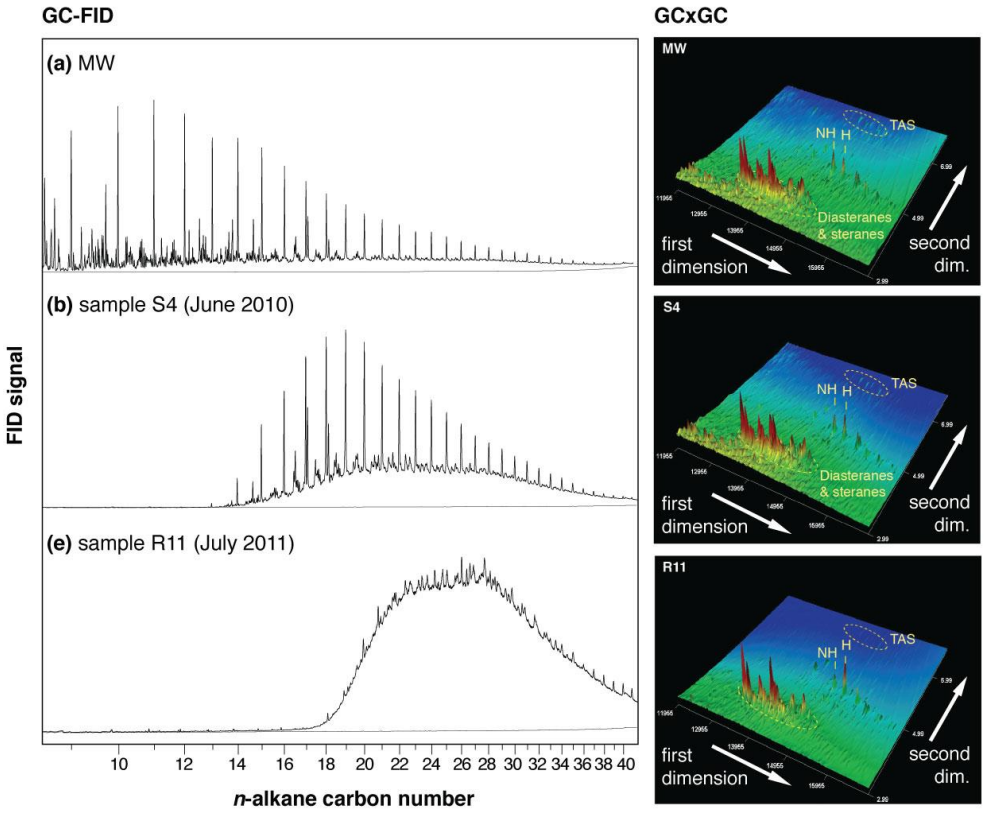

Figure 3. GC-FID (left panels) and the biomarker region of GC×GC chromatograms (right panels) of MW and weathered oil samples, collected from the wellhead, on the sea surface, and on beaches of the Gulf of Mexico. Although the samples were weathered to very different degrees, the biomarker region of the samples remained very similar.

Formation of OxHC due to oil weathering

We found that with increasing weathering, a fraction of non-GC amenable compounds were formed in the weathered oil samples (Figure 4). Elemental, FT-IR, and radiocarbon analysis of this fraction revealed that it consisted of highly oxygenated compounds (average molecular formula was $(C_5H_7O)_n$ with carbonyl and hydroxyl groups), which were formed from petroleum hydrocarbons (Aeppli *et al.* 2012). We therefore refer to this fraction as oxygenated hydrocarbons (OxHC).

The OxHC fraction was persistent on the time scale of this investigation (up to 28 months post-spill), and increased to up to 80% of the total sample mass. The OxHC fraction also correlated with molecular ratios that are indicative of oil weathering, such as the phytane/17α(*H*),21β(*H*)-hopane ratio (Figure 6a). We also linked the formation of OxHC to the disappearance of saturated compounds (Hall *et al.* 2013). This led us to propose to use the relative amount of the OxHC fraction in a given sample as a proxy for its degree of oil weathering (Aeppli *et al.* 2012).

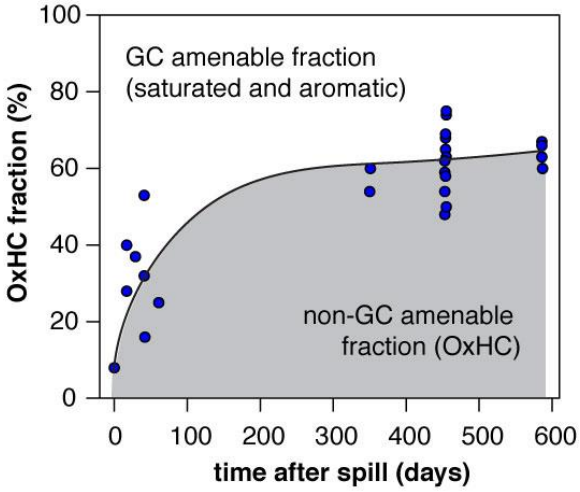

Figure 4. Increase in OxHC fraction with time of weathering. The OxHC fraction is not amenable to gas chromatography (GC).

Physical weathering processes: evaporation and dissolution

Physical oil weathering processes (e.g., evaporation, dissolution) can be easily identified on a GC×GC chromatogram. GC×GC separates compounds according to two different physical properties. The first-dimension column separated according to the vapor pressure of the analytes. Evaporation of compounds in the environment can therefore be identified on the GC×GC chromatogram by removal of compounds with low retention times (i.e, compounds with low *n*-alkane carbon numbers, Figure 5). Dissolution, on the other hand, can be identified on GC×GC by preferential removal of compounds with higher second-dimension retention times. This is because compounds with higher polarity (i.e., water solubility) are more retained on the second-dimension column.

For the investigated samples we saw a moving evaporation front with time of weathering of the samples in the environment. For slick samples, compounds with carbon numbers < 12 were evaporated relative to crude oil (Figure 5a-b). In contrast to these ~1 to 3 cm thick oil slicks, we observed a more rapid evaporation for thin oil sheen that was collected in 2012 at the *Deepwater Horizon* site, with compounds with carbon numbers < 16 were evaporated (Aeppli *et al.* 2013). Evaporation continued once the oil arrived at the beaches (Figure 5c-d).

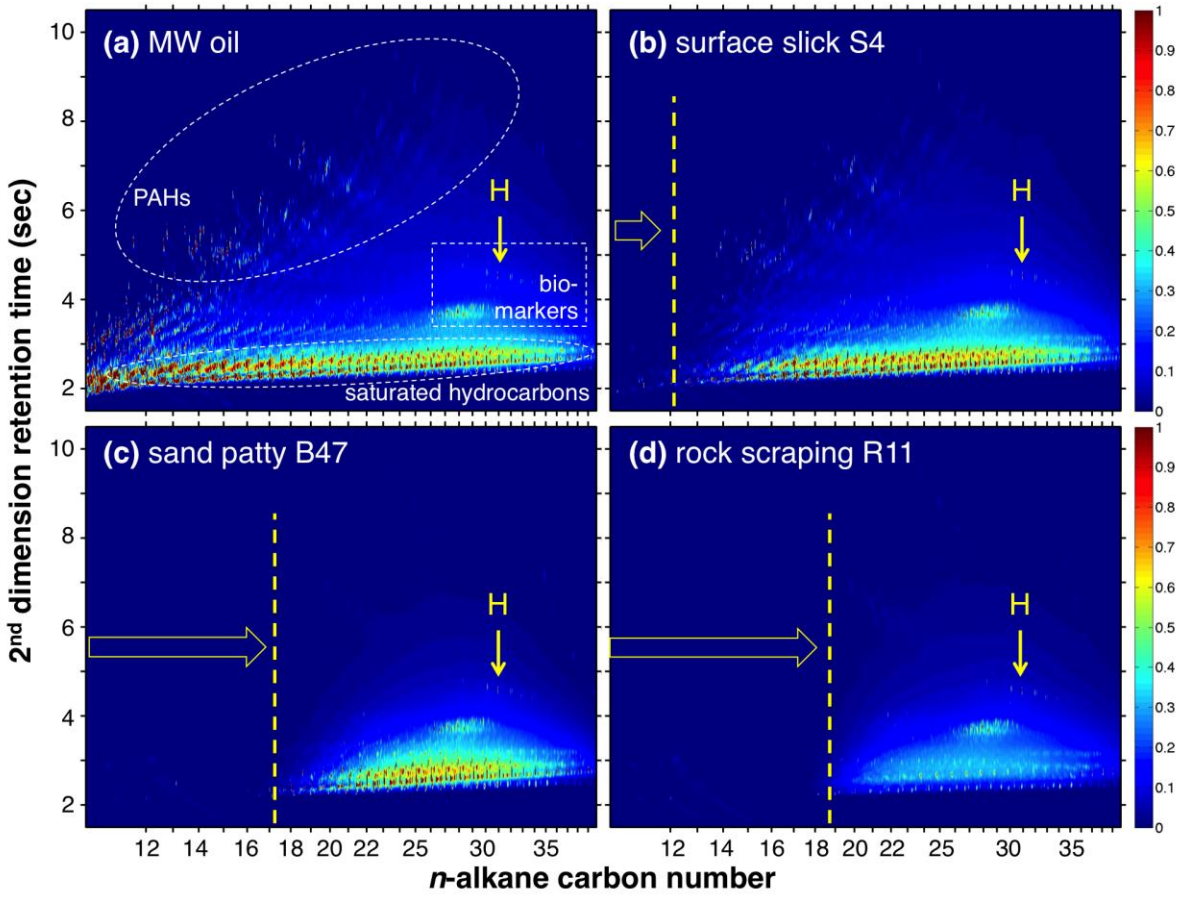

Figure 5. Weathering of MW oil as seen in GC×GC. All chromatograms are normalized to the peak height of 17α(*H*),21β(*H*)-hopane ("H"). With increasing weathering, loss of lighter compounds (evaporation, indicated by horizontal arrows) and selective removal of compounds classes such as PAHs and *n*-alkanes (photooxidation and biodegradation) can be seen.

Biodegradation and photo-oxidation of petroleum hydrocarbons

Beside physical weathering processes, compound-class selective removal of hydrocarbons was observed. This can be seen in a relative disappearance of alkanes and PAHs relative to biomarker compounds (Figure 5).

We investigated to what extent biodegradation, as well as photooxidation, were responsible for this removal of compounds. To this end, we investigated changes in ratios of compounds with the weathering proxy OxHC, and explained this by comparing the physico-chemical properties of the compounds (Figure 6). For example, the decrease of phytane to 17α(*H*),21β(*H*)-hopane (Figure 6a) can be driven by the difference in a variety of physical properties as well as in their biodegradability (Table 1). Therefore, this ratio is not suitable to investigate biodegradation; rather it is a general indication of oil weathering.

In contrast, the ratio of phytane to *n*-octadecane (Figure 6b) is a good indicator of biodegradation, as the major difference in the physico-chemical properties of these two compounds is their susceptibility towards biodegradation (Table 1). For the same reasons, the disappearance of C_{35}-homohopane relative to 17α(*H*),21β(*H*)-hopane (Figure 6c) has to be driven by biodegradation (Aeppli *et al.* 2014).

The concept of comparing two different compounds can also be applied to whole compound classes. By analyzing several alkane compound classes, we found a biodegradation sequence in the order of increasing resistance towards biodegradation of *n*-alkanes > cycloalkanes ≈ methyl-alkanes > cyclic isoprenoids ≈ isopernoids (Gros *et al.* 2014).

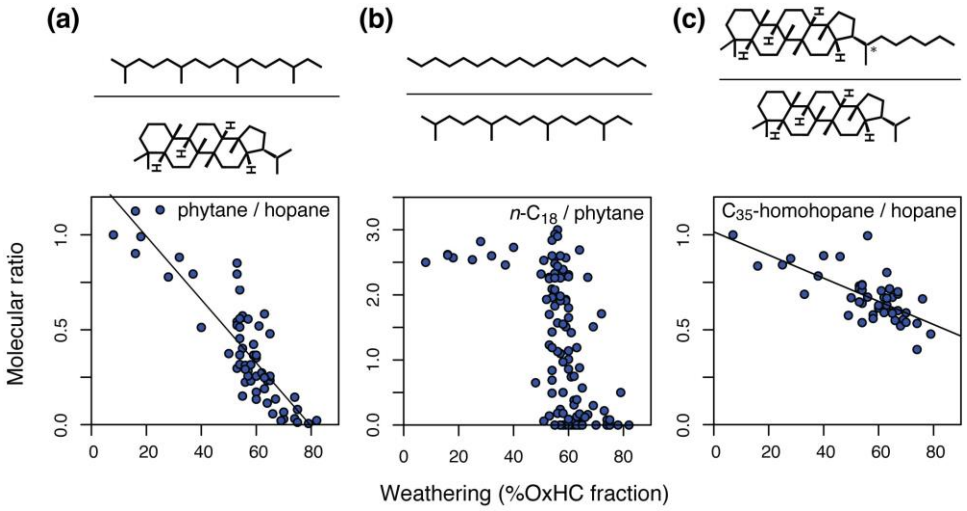

Figure 6. Molecular ratios indicative of oil weathering. (a) Phytane / 17α(*H*),21β(*H*)-hopane is a general indicator of physical as well as bio(chemical) oil weathering. (b-c) The disappearances of *n*-octadecane relative to phytane as well as that of C_{35}-homohopane relative to 17α(*H*),21β(*H*)-hopane are indicative of biodegradation.

Table 1. Physical properties of select alkanes, hopanoids, and aromatic compounds. Vapor pressure (p*), aqueous solubility (C*sat*), and octanol-water partitioning coefficient (K*ow*) were calculated using Sparc v4.6 (http://archemcalc.com/sparc).

Compound	CAS	MW	p*	C*sat*	Log(K*ow*)	Biodegradation
		g mol^{-1}	Pa	mg L^{-1}	Log(M/M)	
Alkanes						
n-C_{17}	1921-70-6	268.5	1.9E-02	2.6E-07	11.1	+++++
pristane	629-78-7	240.5	4.8E-02	3.0E-06	10.1	+++
n-C_{18}	638-36-8	282.6	5.5E-03	6.7E-08	11.6	+++++
phytane	593-45-3	254.5	1.4E-02	6.5E-07	10.6	+++
Hopanoids						
C_{30}-hopane	471-62-5	412.7	5.7E-09	6.2E-13	15.4	-
C_{35}-homohopane	54370-82-0	482.9	2.0E-11	6.1E-16	18.2	+

Aromatic compounds						
chrysene	218-01-9	228.3	1.2E-05	1.2E-02	5.9	++
C_3-chrysene	n/a	270.4	9.9E-07	3.8E-03	7.0	+
C_{20}-TAS	81943-50-21	260.4	1.6E-05	3.6E-03	7.0	++
C_{21}-TAS	n/a	274.4	7.8E-06	1.7E-03	7.4	++
C_{28}-TAS	80382-33-8	372.6	6.7E-09	1.2E-06	10.3	+

In contrast to biodegradation of saturated compounds, we observed photooxidation as the main degradation process for aromatic structures. This can be illustrated by the ratio of chrysene and its C_3-alkylated congeners, which decreases with increasing weathering of the field samples (Figure 7a, and Aeppli *et al.* (2012)). Given the physical properties of chrysene and C_3-chrysenenes (Table 1), the opposite trend in this ratio would be expected if physical processes were responsible for the shift. Likewise, biodegradation is know to be more effective towards chrysene than towards its alkylated congeners (Prince *et al.* 2003). In contrast, photooxidation is more efficient with C_3-chrysene that chrysene, as alkylation activates the aromatic system. The shift in chysene/C_3-chrysene can therefore be explained by photooxidation as the main process leading to depletion of chrysenes.

Note, that lighter PAHs (e.g., naphthalanes, phenanthrenes) are probably also affected by photooxidation. However, these compounds are within the evaporation front (between *n*-C_{12} and *n*-C_{18}; Figures 3a and 5), and are also fairly water-soluble. Consequently, it is challenging to separate the contribution of photooxidation from evaporative and dissolution for these compounds. However, approaches involving numerical modeling would be suitable to do this.

The biomarkers of the triaromatic steroid (TAS) family are also affected by photooxidation. In field samples, we observed a decrease of TAS relative to 17α(*H*),21β(*H*)-hopane (Figure 7b-c); interestingly, this degradation affected various TASs, such as C_{21}-TAS and C_{28}-TAS to the same extent (Radović *et al.* 2013, Aeppli *et al.* 2014). Given that C_{21} and C_{28}-TAS have almost three orders of magnitude difference in physical properties (e.g., aqueous solubility, vapor pressure, octanol-water partition coefficient) (Table 1), evaporation and dissolution can be ruled out as the driver of TAS disappearance. Biodegradation can also be excluded as the main driver of this process, as large differences in biodegradability of various TAS have previously been observed in laboratory incubation experiments (Douglas *et al.* 2012). Given that all TASs have a similarly activated aromatic system, we hypothesize that photooxidation is responsible for the TAS degradation observed for weathered MW oil. To confirm this hypothesis, we performed photooxidation incubations with crude oil, and found a similar TAS degradation across all TAS congeners (Radović *et al.* 2013).

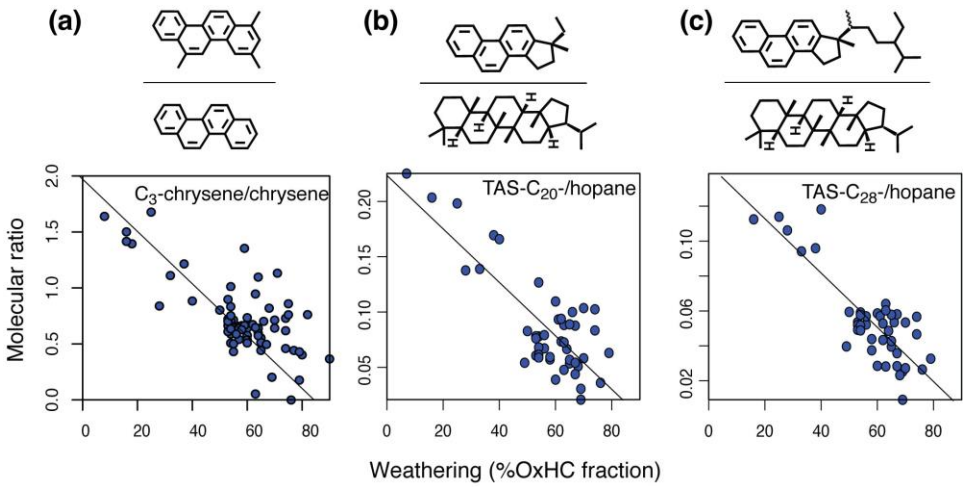

Figure 7. Molecular ratios indicative of photooxidation. (a) C_3-chrysene is preferentially removed relative to chrysene. (b-c) C_{21}-triaromatic steroid (C_{21}-TAS) is removed to relative to hopane to the same extent as C_{28}-TAS, which has very different physical properties as well as susceptibility towards biodegradation.

Our findings suggest that in the investigated samples, straight-chain, branched, and cyclic alkanes were subject to biodegradation, while aromatic compounds were mainly degraded by sunlight. With some exceptions (TAS and homohopanes), biomarker compounds were recalcitrant on the observed time scale of years and are therefore suitable for fingerprinting MW oil.

CONCLUSIONS:

Knowing which constituents in crude oil are either labile or recalcitrant will not only be useful for the development of new oil fingerprinting techniques, but can also help identify novel recalcitrant and potential toxic compounds of concern that should be included in standard monitoring programs after oil spills. In this study, GC×GC was an excellent tool to determine biomarker ratios. Second, this study illustrates that weathering of oil was accompanied by formation of recalcitrant oxygenated transformation products. Although we were able to characterize this fraction on a bulk level in terms of oxygen contend, functional groups and radiocarbon content, these OxHCs are still poorly characterized on a molecular level. Third, analyzing relative disappearance of compounds or compound classes provided evidence that biodegradation, as well as photooxidation, were acting on MW oil.

ACKNOWLEDGEMENT:

This research was made possible in part by grants from the NSF (OCE-0960841, RAPID OCE-1043976, RAPID OCE-1042097, EAR-0950600, OCE-0961725, OCE-1333148), and in part by a grant from BP/the Gulf of Mexico Research Initiative (GoMRI-015) and the DEEP-C consortium.

REFERENCES:

Aeppli, C., Carmichael, C.A., Nelson, R.K., Lemkau, K.L., Graham, W.M., Redmond, M.C., Valentine, D.L. and Reddy, C.M. (2012). *Oil weathering after the Deepwater Horizon disaster led to the formation of oxygenated residues*. Environ. Sci. Technol. **46**(16): 8799-8807.

Aeppli, C., Reddy, C.M., Nelson, R.K., Kellermann, M. and Valentine, D.L. (2013). *Recurrent oil sheens at the Deepwater Horizon disaster site fingerprinted with synthetic hydrocarbon drilling fluids*. Environ. Sci. Technol. **47**(15): 8211-8219.

Aeppli, C., Nelson, R.K., Radović, J.R., Carmichael, C.A. and Reddy, C.M. (2014). *Recalcitrance and degradation of petroleum biomarkers upon abiotic and biotic natural weathering of Deepwater Horizon oil*. Environ. Sci. Technol.: doi:10.1021/es500825q.

Arey, J.S., Nelson, R.K., Plata, D.L. and Reddy, C.M. (2007a). *Disentangling oil weathering using GCxGC. 2. Mass transfer calculations*. Environ. Sci. Technol. **41**(16): 5747-5755.

Arey, J.S., Nelson, R.K. and Reddy, C.M. (2007b). *Disentangling oil weathering using GCxGC. 1. Chromatogram analysis*. Environ. Sci. Technol. **41**(16): 5738-5746.

Atlas, R.M. (1981). *Microbial degradation of petroleum hydrocarbons: An environmental perspective*. Microbiol Rev **45**(1): 180-209.

Carmichael, C.A., Arey, J.S., Graham, W.M., Linn, L.J., Lemkau, K.L., Nelson, R.K. and Reddy, C.M. (2012). *Floating oil-covered debris from Deepwater Horizon: identification and application*. Environ. Res. Lett. **7**: 015301.

Douglas, G.S., Hardenstine, J.H., Liu, B. and Uhler, A.D. (2012). *Laboratory and field verification of a method to estimate the extent of petroleum biodegradation in soil*. Environ. Sci. Technol. **46**(15): 8279-8287.

Eiserbeck, C., Nelson, R.K., Grice, K., Curiale, J. and Reddy, C.M. (2012). *Comparison of GC-MS, GC-MRM-MS, and GCxGC to characterise higher plant biomarkers in Tertiary oils and rock extracts*. Geochim. Cosmochim. Acta **87**: 299-322.

Frysinger, G.S., Gaines, R.B. and Reddy, C.M. (2002). *GC x GC - A new analytical tool for environmental forensics*. Environ. Forensics **3**(1): 27-34.

Garrett, R.M., Pickering, I.J., Haith, C.E. and Prince, R.C. (1998). *Photooxidation of crude oils*. Environ. Sci. Technol. **32**(23): 3719-3723.

Gros, J., Reddy, C.M., Aeppli, C., Nelson, R.K., Carmichael, C.A. and Arey, J.S. (2014). *Resolving biodegradation patterns of persistent saturated hydrocarbons in weathered oil samples from the Deepwater Horizon disaster*. Environ. Sci. Technol. **48**(3): 1628-1637.

Hall, G.J., Frysinger, G.S., Aeppli, C., Carmichael, C.A., Gros, J., Lemkau, K.L., Nelson, R.K. and Reddy, C.M. (2013). *Oxygenated weathering products of Deepwater Horizon oil come from surprising precursors*. Mar. Pollut. Bull. **75**: 140-149.

Nicodem, D.E., Guedes, C.L.B. and Correa, R.J. (1998). *Photochemistry of petroleum I. Systematic study of a brazilian intermediate crude oil*. Mar. Chem. **63**(1-2): 93-104.

Prince, R.C., Garrett, R.M., Bare, R.E., Grossman, M.J., Townsend, T., Suflita, J.M., Lee, K., Owens, E.H., Sergy, G.A., Braddock, J.F., Lindstrom, J.E. and Lessard, R.R. (2003). *The roles of photooxidation and biodegradation in long-term weathering of crude and heavy fuel oils*. Spill Sci Technol B **8**(2): 145-156.

Prince, R.C. and Walters, C.C. (2007). Biodegradation of Oil Hydrocarbons and Its Implications for Source Identification. In *Oil Spill Environmental Forensics - Fingerprinting And*

Source Identification. Z. Wang and S. A. Stout (Eds.). Burlington MA, San Diego CA, London U.K., Academic Press**:** 349-379.

Radović, J.R., Aeppli, C., Nelson, R.K., Jimenez, N., Reddy, C.M., Bayona, J.M. and Albaiges, J. (2013). *Assessment of photochemical processes in marine oil spill fingerprinting*. Mar. Pollut. Bull. **79**: 268–277.

Short, J.W., Irvine, G.V., Mann, D.H., Maselko, J.M., Pella, J.J., Lindeberg, M.R., Payne, J.R., Driskell, W.B. and Rice, S.D. (2007). *Slightly weathered Exxon Valdez oil persists in Gulf of Alaska beach sediments after 16 years*. Environ. Sci. Technol. **41**(4): 1245-1250.

Wang, Z., Yang, C., Fingas, M., Hollebone, B., Yim, U.H. and Oh, J.R. (2006). Petroleum biomarker fingerprinting for oil spill characterization and source identification. In *Oil Spill Environmental Forensics - Fingerprinting And Source Identification*. Z. Wang and S. A. Stout (Eds.). Burlington MA, San Diego CA, London U.K., Academic Press**:** 73-146.